

## ORIGINAL RESEARCH

# Effects of greenhouse gas emissions timing on alternative biomass and fossil energy sources for district heating

Saurajyoti Kar<sup>1</sup>  | Pieter Billen<sup>2</sup>  | Lars Björnebo<sup>1</sup> | Beth Katz<sup>3</sup> | Sheng Yang<sup>4</sup>  | Timothy A. Volk<sup>4</sup>  | Sabrina Spatari<sup>1,5</sup> 

<sup>1</sup>Civil, Architectural & Environmental Engineering, Drexel University, Philadelphia, Pennsylvania, USA

<sup>2</sup>Intelligence in Processes, Advanced Catalysts & Solvents (iPRACS), Faculty of Applied Engineering, University of Antwerp, Antwerp, Belgium

<sup>3</sup>Chemical and Biological Engineering, Drexel University, Philadelphia, Pennsylvania, USA

<sup>4</sup>College of Environmental Science and Forestry, State University of New York, Syracuse, New York, USA

<sup>5</sup>Faculty of Civil and Environmental Engineering, Technion—Israel Institute of Technology, Haifa, Israel

## Correspondence

Sabrina Spatari, Faculty of Civil and Environmental Engineering, Technion—Israel Institute of Technology, Haifa, Israel.  
Email: ssabrina@technion.ac.il; ss3226@drexel.edu

## Funding information

USDA National Institute of Food and Agriculture, Grant/Award Number: 2012-68005-19703

## Abstract

District heating (DH) systems can improve energy efficiency, reduce greenhouse gas (GHG) emissions, and be a cost-effective residential space heating alternative over conventional decentralized heating. This study uses radiative forcing (RF), a time-sensitive life cycle assessment metric, to evaluate space heating alternatives. We compare forest residue and willow biomass resources and natural gas as fuel sources against decentralized heating using heating oil. The comparison is performed for selected locations in the Northeastern United States over a 30-year production timeline and 100 observation years. The natural gas and willow scenarios are compared with scenarios where available forest residue is unused and adds a penalty of GHG emissions due to microbial decay. When forest residues are available, their use is recommended before considering willow production. Investment in bioenergy-based DH with carbon capture and storage and natural-gas-based DH with carbon capture and storage (CCS) technology is considered to assess their influence on RF. Its implementation further improves the net carbon mitigation potential of DH despite the carbon and energy cost of CCS infrastructure. Soil carbon sequestration from willow production reduces RF overall, specifically when grown on land converted from cropland to pasture, hay, and grassland. The study places initial GHG emissions spikes from infrastructure and land-use change into a temporal framework and shows a payback within the first 5 years of operation for DH with forest residues and willow.

## KEYWORDS

BECCS, bioenergy crops, CCS, district heating, LCA, radiative forcing, temporal GHG emissions

## 1 | INTRODUCTION

Building space heating infrastructure comprises a large fraction of residential energy consumption, constituting a record 57% of total household energy in the

Northeastern United States, where heating oil supplies 20% of the energy demand (USEIA, 2015). With its cold and mixed-humid climate, the U.S. Northeast region requires permanent heating infrastructure for residential and commercial buildings. According to the U.S. Energy

This is an open access article under the terms of the Creative Commons Attribution License, which permits use, distribution and reproduction in any medium, provided the original work is properly cited.

© 2021 The Authors. *GCB Bioenergy* published by John Wiley & Sons Ltd.

Information Administration, this region consumes 84% of the total heating oil (about  $43 \times 10^9$  L) used in the United States, representing a significant dependence on liquid fossil fuel (USEIA, 2015). In recent years, several initiatives to diversify fuel supply have been undertaken worldwide (European Commission, 2018) and specifically in the United States (CARB, 2013). Among those strategies, biomass is a viable heating energy source due to its local availability and cost-effectiveness when replacing heating oil in rural areas (Wilson et al., 2012).

Recently proposed and implemented (CARB, 2012, 2013) energy policies require, and in some cases incentivize, the use of low-carbon and renewable energy to mitigate climate change by reducing atmospheric greenhouse gas (GHG) emissions (Chu & Majumdar, 2012). Achieving those policy targets requires using low-carbon fuels, updating current infrastructure to reduce GHG emissions or both. To achieve low-carbon policy targets in residential heating, regions in the Northeastern United States with existing natural gas pipeline infrastructure can benefit from switching to natural gas. Natural gas has lower combusive GHG emissions per unit of delivered energy ( $50 \text{ g CO}_2\text{e MJ}^{-1}$ ) compared to heating oil ( $70 \text{ gCO}_2\text{e MJ}^{-1}$ ; USEPA, 2020). Its higher heating value ( $52 \text{ MJ kg}^{-1}$ ) is also greater than that of heating oil ( $46 \text{ MJ kg}^{-1}$ ), delivering more thermal energy per unit mass to satisfy a given heat demand. However, methane leakages during natural gas extraction and distribution (Brandt et al., 2016), which are equivalent to 2.3% of yearly gross U.S. natural gas production, are also a disadvantage of the resource (Alvarez et al., 2018). Replacing natural gas with biomass can lower fossil-fuel-related GHG emissions by restricting their emission to transportation and logistics processes and avoiding the end-use emissions when fossil fuels are used for heating.

Sustainably sourced woody biomass is a promising alternative to fossil energy for heat and power generation (Langholtz et al., 2016; McKendry, 2002). Life cycle assessment (LCA) studies have estimated that using biomass as sole or co-fed feedstock for combined heat and power (CHP) production and district heating infrastructures (DH) has environmental benefits (Dias et al., 2017; McManus, 2010; Parajuli et al., 2015; Zuwała, 2012). High-resolution mapping of the United States' aboveground woody biomass has helped visualize the vast availability of woody biomass areas in the Northeast regions (Kellndorfer et al., 2013). Timber production regularly utilizes some of the woody biomass of the region. However, the residues from the portions of harvested trees, such as tops and branches, are left unused to decay on forestland. If collected, woody biomass residues can serve as feedstock for space heating.

An alternative to forest residues, short-rotation crops such as willow, are potential low-carbon feedstocks for heating applications (Volk et al., 2016). Carbon

sequestration from willow crop roots and belowground stool can reduce net GHG emissions (Pacaldo et al., 2013). Nevertheless, growing willow may invoke direct land-use change (LUC), and indirect land-use change (ILUC)-related GHG emissions owing to changes in aboveground and belowground carbon stocks (Searchinger et al., 2008). The positive (decreased) or negative (increased) impact on atmospheric GHG emissions depends on historical land-use practices of the transformed land. Positive and high in magnitude LUC GHG emissions can adversely impact the overall GHG balance of willow biomass, diminishing its low-carbon advantages from soil carbon sequestration (Havlik et al., 2011). However, feedstock crops cultivated on marginal land and land not planned for long-term agricultural use can mitigate ILUC-based GHG emissions (Gelfand et al., 2013; Zumkehr & Campbell, 2013).

Life cycle assessment studies that consider fixed-time horizons usually aggregate all GHG emissions are over time, for example, over 100 years (Jørgensen & Hauschild, 2013), ignoring the magnitude and temporal sequence of those emissions within the product life cycle (Levasseur et al., 2016). Today's emissions have a more substantial adverse environmental impact than tomorrows. This is because a fraction of today's emissions will persist in tomorrow's atmosphere. Resolving the temporal GHG emissions from foreground and background processes found in ecoinvent 2.2 datasets for several product life cycles, Pinsonnault et al. (2014) found the global warming impacts for bioenergy systems to show most sensitivity compared to other products, heightening the need to consider the timing of emissions occurring from biofuel and biomass-based processes. Furthermore, LUC-related GHG emissions from short-rotation crops are temporally asynchronous, which can significantly affect the payback time from using biomass rather than fossil fuel. This highlights the need for temporal accounting of GHG emissions for comparing biomass use with conventional energy feedstocks in heating infrastructures in bioenergy policy decisions (Pingoud et al., 2012; Pourhashem et al., 2016).

O'Hare et al. (2009), Kendall et al. (2009), and Levasseur et al. (2010) were among the first studies that developed approaches to temporal accounting of GHG emissions (Kendall et al., 2009; Levasseur et al., 2010; O'Hare et al., 2009). O'Hare et al. (2009) developed a temporal accounting method of GHG emissions using  $\text{CO}_2$  decay captured in the Bern cycle. They posit that this method is analogous to economic discounting of  $\text{CO}_2$  emissions in future years, to compare irregular  $\text{CO}_2$  emissions in a crop-based biofuel product compared to the more regular GHG emissions of conventional gasoline use for transportation. Their method finds that early emissions in a time horizon cause a higher radiative effect compared to later emissions. Kendall et al. (2009) developed a time

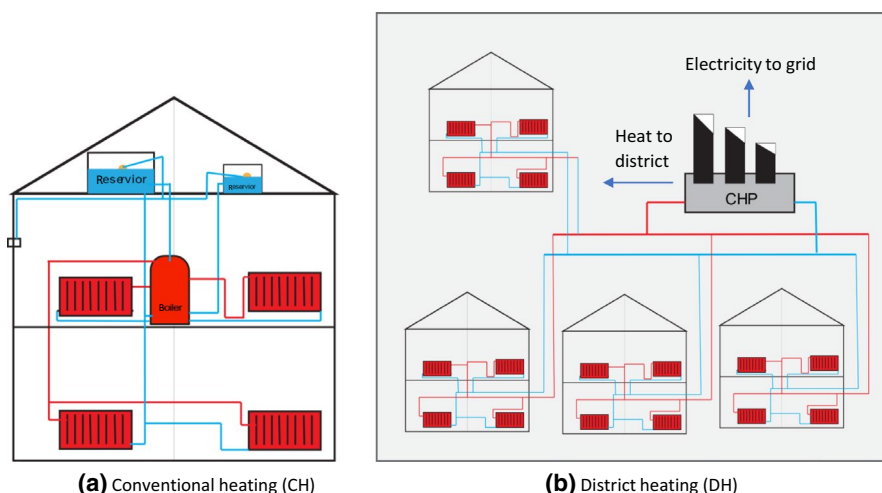
correction factor to account for time effects of GHG emissions from LUC, using cumulative radiative forcing (CRF). Schwietzke et al. (2011) implemented a time-based radiative forcing (RF) method to assess the influence of continuously increasing corn-ethanol production in the United States due to the Renewable Fuel Standard government mandate, highlighting a significant reduction over gasoline baseline RF estimates for minimum LUC emissions (Schwietzke et al., 2011). However, those GHG reduction benefits varied with varying analysis timeframes while considering the expansion of corn for ethanol cultivation. When uncertainty in indirect LUC emissions is considered, it overshadows the benefits of reducing GHG emission, as otherwise highlighted by the temporal accounting approach, by one to two orders of magnitude. Cherubini et al. (2011) developed a time-sensitive global warming potential metric ( $GWP_{bio}$ ) that considers temporal pulse GHG emissions and atmospheric persistence of GHGs for varying durations including 20-, 100-, and 500-years' time horizons. Another study by the same authors developed a spatially explicit analysis of forest biomass use showing that global warming (in  $gCO_2$  eq.) increases with longer forest turnover times as well as with larger amounts of left-over forest residues (Cherubini et al., 2016). Schivley et al. (2015) performed a time-series analysis of GHG reduction for a coal-fired power plant and report that co-firing with biomass can reduce the life cycle impact (Schivley et al., 2015). Overall, studies that use temporal accounting methods have elucidated details on climate change impact, elaborating on trends over time as well as at specific points when GHG concentrations shift and introduce an inflection point, reflecting a change in RF.

In addition to replacing fossil fuel with biomass-based energy sources, bioenergy with carbon capture and storage (BECCS) is recognized as a key strategy for limiting global warming to  $2^\circ C$  (Fuss et al., 2018). Thus, we compare BECCS used in biomass-DH with carbon capture

and storage (CCS) added to natural gas-DH infrastructure. Post-combustion CCS technology acts to arrest  $CO_2$  from flue gas and transport it by pipeline for storage in geologic formations (Rhodes & Keith, 2005; Volkart et al., 2013). We investigate the effect of CCS technology on RF as a function of time for natural-gas-based and biomass-based DH.

This study aims to apply a temporal analysis method to compare alternative residential heating infrastructures—conventional and DH—for feedstocks with asynchronous emissions. Given that DH requires investment in infrastructure, ongoing consumption of feedstock, and possible use of CCS/BECCS over a time horizon in which the investment is applied, temporal accounting of GHG emissions aims to understand the pattern of GHG emissions and major shifts at specific time junctures when an investment is made or a change occurs related to the GHG emissions, such as LUC. A conventional heating (CH) infrastructure consists of independent heating units located at each individual location, that is, buildings. In contrast, DH infrastructure consists of a centralized CHP plant for residences in neighborhoods supplied with heated water or steam through insulated pipes for space heating purposes. The production of both heat and power vastly improves the efficiency of energy delivery in DH systems and reduces the net GHG emissions owing to co-produced electricity, which is credited via LCA (Björnebo et al., 2018). Figure 1 shows a schematic representing CH and DH infrastructures. We use the RF LCA midpoint indicator to measure the time-sensitive environmental impact, measured in  $Watts\ m^{-2}\ MWh^{-1}$ . RF captures the change in environmental GHGs as changing amounts of heat energy in Earth's atmosphere. It has been used in other temporal emissions studies (Levasseur et al., 2010; Pourhashem et al., 2016). Its importance as a midpoint indicator within the climatic cause-effect life cycle chain has been highlighted in a recent review in Levasseur et al. (2016). In addition, we use a metric that relates the CRF with a baseline

**FIGURE 1** Schematics of (a) conventional heating (CH) and (b) district heating (DH) infrastructures. In CH, the feedstock is combusted to produce heated water in the boiler, which is then circulated through pipes within the house. Whereas, in DH, a centralized conventional heat and power plant (CHP) circulates residual heat to neighboring residences through insulated pipes for space heating



scenario and pulse emission. To our knowledge, this study is the first to combine temporal emissions modeling for comparing residential heating infrastructures, feedstock alternatives, and the addition of CCS.

## 2 | BACKGROUND

This research builds on the LCA and GHG abatement framework for DH investment studied by Björnebo (2015) and Björnebo et al. (2018), who identified 10 economically feasible locations, each with and without natural gas pipeline infrastructures, for implementing DH in New England, USA (Table 1). The authors used location-specific hourly heat load demand and system energy efficiency data with CHP and DH equipment optimization to estimate feedstock choices by location (Henning, 1998, 1999; Henning et al., 2006). Björnebo et al. include heat demand estimation and plant dimensioning to calculate future investment while considering installation costs. The authors perform a detailed LCA of DH systems employing natural gas and biomass, finding a sharp reduction in GHG emissions due to efficiency and electricity displacement credits compared to centralized heating. The selected locations for DH application have a negative GHG abatement cost (Table 1). We consider the locations with natural gas pipelines to use natural gas-based CH or DH. Locations that do not have natural gas pipelines but have negative GHG abatement costs are considered preferable for forest biomass-based DH.

## 3 | METHODS

We compare the RF resulting from GHG emissions from CH and DH heating scenarios. We assume CH

infrastructure is pre-installed at the locations of interest. Hence, we do not consider sunk GHG emissions from past installations. Whereas DH requires installation; hence its GHG emissions are included. In a DH system, the auxiliary heat from a CHP plant is the heat source. A piping network to the district's residential buildings circulates heated water or steam.

Table 2 lists the scenarios compared in this study. CH and DH are two residential infrastructure choices compared with heating oil, natural gas, forest residues, and willow short-rotation crop feedstocks. We include scenarios where CCS is applied to combustive CO<sub>2</sub> emissions. Different scenarios examine the influence of belowground soil carbon change from willow growth on the RF profile. When unused, forest residue decays naturally, emitting CO<sub>2</sub> to the atmosphere. We compare scenarios that include and exclude the GHG emissions from the natural decay of unused forest residues to assess the CO<sub>2</sub> cost of avoiding the natural decay of biomass when forest residues are available and used in heating infrastructures. Willow short-rotation crop requires additional land management. Forest residue is economically favorable if available before investing in willow as feedstock. The scenarios studied here highlight the environmental cost of not using forest residues, even if available. The scenarios are compared using a unified timeline (Section 3.1).

### 3.1 | GHG Emission timeline and LCA boundary

We use the IPCC 100-year analysis method to estimate GHG emissions (Kaito et al., 2014). We calculate the RF effect of CO<sub>2</sub>, CH<sub>4</sub>, and N<sub>2</sub>O gases, over a 100-year time horizon that includes the first 30 years of heating

**TABLE 1** Heat demand for 10 economically feasible and cost-effective conventional heating and district heating systems by locations with and without access to natural gas pipelines

Natural gas available locations, state	Heat demand ×10 <sup>4</sup> MWh year <sup>-1</sup>	Forest residue available locations, state	Heat demand ×10 <sup>4</sup> MWh year <sup>-1</sup>
Granby CDP, MA	5.8	Waldoboro CDP, ME	11.5
Townsend CDP, MA	4.9	Amherst CDP, NH	5.1
Dover CDP, MA	9.0	Hartland CDP, VT	2.8
Norton Center CDP, MA	6.0	Plattekill CDP, NY	11.4
Gardiner city, ME	21.8	Brownville, NY	9.2
Groton CDP, MA	10	Schaghticoke, NY	4.4
Monson Center CDP, MA	13.2	Schuylerville, NY	9.6
Rowley CDP, MA	8.3	Alton CDP, NH	4.7
Freeport CDP, ME	7.2	Gardiner CDP, NY	7.1
Belchertown CDP, MA	13.3	Fort Ann, NY	2.9

Source: Data adapted from table 4 in Björnebo et al. (2018).



**TABLE 2** A summary list of scenarios for analysis. Scenario abbreviations presented here are utilized to explain results

Infrastructure	Feedstock	Scenario includes (yes) or excludes (no) forest residue decay	BECCS or CCS enabled (yes/no)	Scenario abbreviation
Conventional (decentralized) heating, CH	Heating oil, HO	No	No	CH-HO
		Yes		CH-HO-Bdecay
	Natural gas, NG	No		CH-NG
		Yes		CH-NG-Bdecay
District (centralized) heating, DH	Natural gas, NG	No	No	DH-NG
			Yes	DH-NG-CCS
		Yes	No	DH-NG-Bdecay
			Yes	DH-NG-Bdecay-CCS
	Forest residue, BM	N/A	No	DH-BM
			Yes	DH-BM-CCS
	Willow, W	No	No	DH-W-CW
				DH-W-PHG
				DH-W-CW-Bdecay
				DH-W-PHG-Bdecay
		Yes	Yes	DH-W-CW-CCS
				DH-W-PHG-CCS
				DH-W-CW-Bdecay-CCS
				DH-W-PHG-Bdecay-CCS

Abbreviations: BECCS, bioenergy with carbon capture and storage; CCS, carbon capture and storage; CH, conventional heating; DH, district heating.

infrastructure operation. Experts recommend considering a 100-year planning horizon for evaluating GHG emissions in near-future policies (Myhre et al., 2013; Shine, 2009). Also, considering 100-year time horizon matches with other studies that perform impact assessment using aggregation approach and IPCC GWP 100a metric.

### 3.1.1 | Natural gas

The preferred locations for natural gas (Table 1) have existing distribution pipelines, needing no new natural gas pipeline infrastructure. Hence, we do not consider emissions from natural gas extraction, treatment, and transportation for CH and DH scenarios. We consider GHG emissions from natural gas use for the 30 production years for natural gas with CH. For DH, we consider GHG emissions from DH installation at the start of production, GHG emissions from natural gas extraction, and natural gas consumption for 30 production years.

### 3.1.2 | Forest residue

Forest biomass residues left unused in the forest undergo slow natural decay through heterotrophic respiration by microorganisms (Palviainen et al., 2004; Vávřová et al.,

2009). Palviainen et al. (2004) found a positive correlation between the natural decay rate and the high initial concentrations of atmospheric carbon and nitrogen within forest residues (Palviainen et al., 2004). The complete natural decay and release of stored carbon take years compared to the immediate release of GHGs by combustion. We assume GHG emissions related to forest residue decay occur over 100 years when forest residues, although available, are not used as feedstock during the 30-year production period. When forest residue supplies DH infrastructure, our calculations consider the GHG emissions from the collection, transportation, and use every production year.

### 3.1.3 | Willow

Preparing existing cropland or pasture, hay, and grassland for willow cultivation requires 1 year, followed by 3–4 years of growth before harvesting (Pacaldo et al., 2013; Volk et al., 2016). We assume 3-year rotation periods for growing willow crops for analysis purposes, allowing annual availability from 3 consecutive land plots (Heller et al., 2003). Some studies confirm a 10%–20% increase per generation of willow yield (Verwijst, 2001). We assume a fixed willow feedstock demand for the heating infrastructures, with the planted willow cultivation able to meet the stationary yearly location-specific demand along the 30

production years. Fertilizer is applied at the first spring season of every 3-year cropping cycle.

We consider GHG emissions from 4 years of land preparation, with the fourth year overlapping the (0th year) infrastructure installation year and followed by the next 30 production years. Soil carbon change-related GHG emissions (data sources described in Section 3.2) from the land transition are quantified separately for the 2nd, 3rd, 4th–6th, and 7th–30th years (Heller et al., 2003). We consider below-ground soil carbon change for 100 centimeters of soil depth. We include harvesting, chipping, and transportation-related emissions for each production year. CO<sub>2</sub> uptake during willow growth is aggregated for each production year.

The additional 4-year land preparation time for willow cultivation extends our overall observation timeframe to 104 years. Figure 2 shows the unified timescale comparing the different residential heating cases with different feedstocks, natural decay of forest residues, and CCS.

We add the GHG emission balances unified over a time series by year (*y*) to obtain the GHG emissions inventory, represented in Equation (1). The negative sign for CCS of CO<sub>2</sub> ( $E_{CCS,g,f,h,y}$ ) from flue gas represents the CO<sub>2</sub> sequestered by CCS technology. Section 3.2 describes the data sources used in this study.

$$E_{g,f,h,y} = \sum (E_{SOC,g,f,h,y} + E_{infr,g,f,h,y} + E_{prod,g,f,h,y} + E_{fr,g,f,h,y} + E_{CCS,g,f,h,y}) \quad (1)$$

$E_{g,f,h,y}$  = yearly greenhouse emission for GHGs, infrastructure, and heating scenario, grams ;

$E_{SOC}$  = greenhouse emission from change in soil organic carbon, grams

$E_{infr}$  = infrastructure installation based greenhouse gas emission, grams ;

$E_{prod}$  = heat production based greenhouse gas emission from feedstock use, grams ;

$E_{fr}$  = greenhouse gas emission from decay of unused forest residues, grams ;

$E_{CCS}$  = Carbon Capture and Storage of CO<sub>2</sub> from flue gas ;  
g = greenhouse gas, CO<sub>2</sub>, N<sub>2</sub>O, or CH<sub>4</sub>; f = heating feedstock;  
h = heading infrastructure; y = production year.

### 3.2 | Data sources and LUC accounting

Figure 3 visualizes the RF model calculation steps along with the data inputs. The life cycle GHG emissions data are based on life cycle inventory models developed by Björnebo et al. (2018) for the production and transportation processes for CH and for the DH infrastructure installation. Direct LUC GHG emissions from cropland transformation are included in the analysis. Direct LUC GHG emissions data are obtained from the carbon calculator for land-use change (CCLUB) tool (Dunn et al., 2013, 2017). CCLUB tabulates yearly soil organic carbon change from LUC simulated by the CENTURY model's SCSOC sub-model developed by Kwon and Hudson (2010). The SCSOC sub-model estimates soil organic carbon changes based on nonlinear soil kinematics equation, nutrient recycling, plant growth, mass balance, and underground water hydraulics. Also, Kwon and Hudson (2010) validate the estimates with the CENTURY model's simulation values. The CENTURY model was developed based on data from agricultural lands in the upper Midwest USA and 30 years of Swedish field experiments (Paustian et al., 1992; Pedersen et al., 2004). Since the current study performs a temporal analysis of emissions, the annual below-ground soil carbon change emissions are converted to the

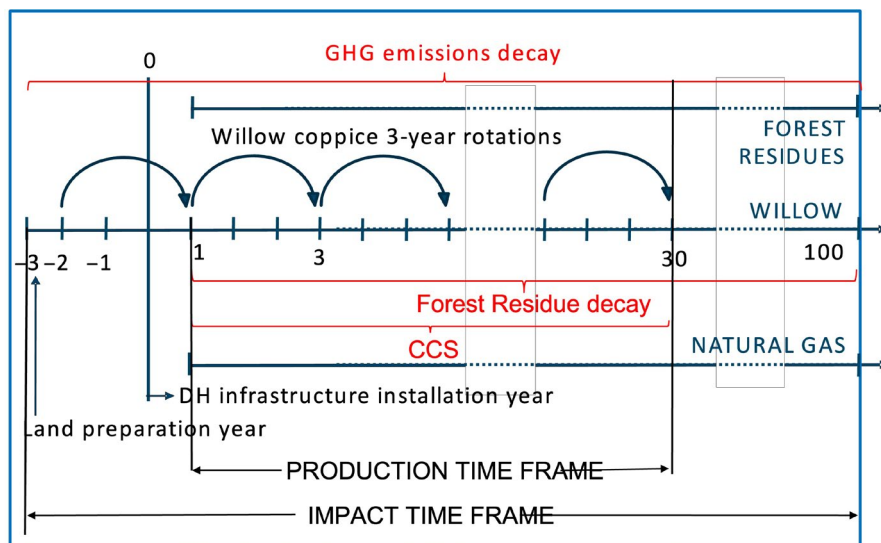


**FIGURE 2** Unified timeline showing the different stages of the analysis for three feedstocks. The short-rotation crop requires 1 year for land preparation and 3 years for crop growth and harvest. Infrastructure-related emissions are added in the 0th year. The 30 years of production are followed by GHG emissions present in the atmosphere, observed for the next 70 years. CCS is assumed to be active for 30 years of production. CCS, carbon capture and storage; DH, district heating; GHG, greenhouse gas

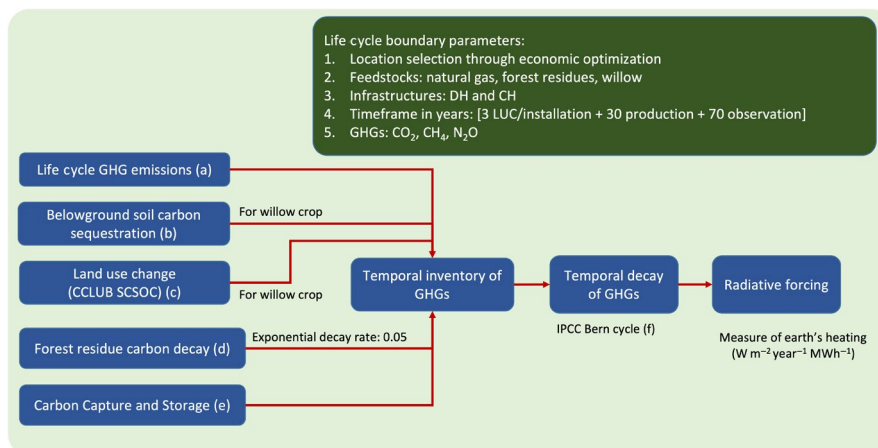


**FIGURE 3** Model components and data flow within the life cycle boundary for the comparative analysis of CH and DH scenarios. RF is estimated as a function of time. The letters referred to in the figure are marked for data sources and methods: (a) economic and environmental optimization study for location set per feedstock use and life cycle GHG emissions modeling (Björnebo et al., 2018), (b) belowground soil carbon sequestration for willow crop plantation (Pacaldo et al., 2013), (c) land-use change-based GHG emissions for growing willow crop (Dunn et al., 2017) and adapting to a temporal scale (O'Hare et al., 2009), (d) natural decay of forest residues releasing the carbon after microbial oxidation (Harmon et al., 2000), (e) CO<sub>2</sub> capture and storage, and energy penalty from CCS (Saint-Pierre & Mancarella, 2014), and (f) application of Bern model to atmospheric GHG decay for the temporal GHG emissions data (Cherubini, Peters, et al., 2011; Forster et al., 2007; Levasseur et al., 2010). CCS, carbon capture and storage; CH, conventional heating; DH, district heating; GHG, greenhouse gas; RF, radiative forcing

temporal scale, using the approach described in Davidson and Ackerman (1993) and O'Hare et al. (2009). Of all the belowground soil carbon lost, 80% is assigned to the first 5 years equally and the remaining 20% to the remaining 95 years. We do not account for aboveground GHG emissions and aboveground soil carbon change from historic land use in our calculation of direct LUC GHG emissions. For example, historic GHG emissions from grasslands used for grazing livestock prior to year 0 in the time horizon defined are not included in our time-series dataset as we assume that to be the carbon burden of historical grassland use.

We implement an exponential decay function for forest residue to represent its natural decay with  $-0.05$  as the decay constant based on one-time regression analysis for birch species in a study by Harmon et al. (2000). That study considered the decay dynamics for several tree species in northwest Russian forests, which have cooler summers than the Northeastern United States. Higher average monthly temperatures in the Northeastern United States should facilitate more rapid decay. Hence, we consider the highest decay rate to represent our diverse species' forest residue decay among the three experimentally studied species in Harmon et al. (Table 2; Harmon et al., 2000).

We assume post-combustion CCS technology's implementation increases installation-based emissions by 30%, considering a 10% higher uncertainty over the 20% value estimated by Singh et al. (2011). We consider CCS a carbon emission reduction technology for the centralized DH

facilities only as it is not practical for decentralized CH. CCS with the monoethanolamine solvent-based CO<sub>2</sub> extraction process has an approximate 90% efficiency in capturing CO<sub>2</sub> in the flue gas. Such efficiency is considered realistic with existing technology as studied by Gelfand et al. (2020), Kunze and Spliethoff (2012), Middleton and Bielicki (2009), and Saint-Pierre and Mancarella (2014) and suggested in IPCC 2005 projections (Metz et al., 2005). Additional energy demand for CCS operations is assumed available from onsite CHP plants at DH facilities. We apply the energy penalties, reported by Saint-Pierre and Mancarella (2014), consist of solvent regeneration (1.25 MWh tCO<sub>2</sub><sup>-1</sup>), CO<sub>2</sub> compression (0.07 MWh tCO<sub>2</sub><sup>-1</sup>), and auxiliary power (0.043 MWh tCO<sub>2</sub><sup>-1</sup>). We assume sufficient biomass and natural gas feedstocks are available to satisfy the additional energy demand from CCS implementation. CO<sub>2</sub> emissions from CCS energy penalties are also considered available for carbon storage. A detailed CCS process description for heat and power plants is available in the literature (Moser et al., 2011; Rubin & Zhai, 2012; Volkart et al., 2013). The change in CO<sub>2</sub> concentration in the atmosphere due to CCS is considered annually for the 30 years of space heating.

### 3.3 | GHG emission decay and RF

The temporal RF calculation presented in this study is adapted from Schwietzke et al. (2011) as it provides

a stepwise approach to expand the temporal analysis framework across multiple scenarios. We calculate the yearly GHG emissions and carbon uptake from the atmosphere by crops as per Equation (1). Furthermore, the Bern model-based GHG emissions decomposition is implemented on life cycle inventory data to calculate the net sustained atmospheric GHG emissions in the atmosphere (Cherubini et al., 2011; Strassmann & Joos, 2018). Equation (2) represents the total atmospheric GHG emissions change (either positive or negative) as a function of different greenhouse gases, feedstock, heating infrastructure, and the study year. The persistent emission<sub>g,f,h,y</sub> component of Equation (2) is calculated by applying the Bern model, as per Equation (3). Next, the GHG emission effect is studied using RF.

$$E_{\text{total,g,f,h,y}} = E_{\text{yearly,g,f,h,y}} + E_{\text{pers,g,f,h,y}}, \quad (2)$$

$$E_{\text{pers,g,f,h,y}} = \sum_{t=0}^{y-1} f_{\text{Bern}}(E_{\text{yearly,g,f,h,t}}), \quad (3)$$

$E_{\text{total}}$  = total greenhouse gas emission, grams ;

$E_{\text{pers}}$  = persistent greenhouse gas emission from the last years, grams ;

$f_{\text{Bern}}$  = function calculating persistent greenhouse gas as per bern cycle model

We aggregate CO<sub>2</sub>, CH<sub>4</sub>, N<sub>2</sub>O GHGs influence into CO<sub>2</sub> equivalence with each gas's atmospheric residence function (Forster et al., 2007). Equation (4) describes the RF calculation, where emission factor<sub>g</sub> represents the GHGs specific radiative efficiencies based on CO<sub>2</sub> equivalence with values of  $1.42 \times 10^{-2}$ , 0.37, and 3.03 Watts m<sup>-2</sup> ppm<sup>-1</sup> for CO<sub>2</sub>, CH<sub>4</sub>, N<sub>2</sub>O GHGs, respectively.

$$\text{RF}_{f,h,y} = \sum_g E_{\text{total,g,f,h,y}} \times \Delta_g \times R_g, \quad (4)$$

RF = radiative forcing from greenhouse gas emission, ; watt m<sup>-2</sup> MWh<sup>-1</sup>

$\Delta_g$  = change in atmospheric concentration of GHGs, ppm g<sup>-1</sup> ;

$R_g$  = emission factor for GHGs, watt m<sup>-2</sup> ppm<sup>-1</sup>.

In addition to assessing the RF over observation years, we calculate the relative change in CRF of alternative residential heating scenarios compared to the heating oil CH-baseline scenario. The global warming factor (GWF) formulation is similar to the GWP metric. However, it is estimated for every production year to realize the temporal

change over 100 observation years. GWF also represents the number of orders of magnitude change over 1 kg pulse CO<sub>2</sub> emission every 30 production years. Equation (5) calculates the GWF for the studied scenarios. A similar mathematical approach is considered to define the ILUC factor by Kløverpris and Mueller (2013).

$$\text{GWF}_{f,h,y} = \frac{\text{CRF}_{f,h,y} - \text{CRF}_{\text{baseline,y}}}{\text{CRF}_{\text{CO}_2\text{pulse,y}}}, \quad (5)$$

GWF<sub>y</sub> = global warming factor calculated yearly, MWh<sup>-1</sup> ;  
 CRF<sub>f,h</sub> = cumulative radiative forcing for feedstock f and infrastructure h ;  
 CRF<sub>baseline</sub> = cumulative radiative forcing for heating oil conventional hating scenario ;  
 CRF<sub>CO<sub>2</sub>pulse</sub> = cumulative radiative forcing from 1 kg CO<sub>2</sub> yearly pulse emission

The temporal modeling to assess RF for scenarios listed in Table 2 is performed using the R programming environment (R Core Team, 2018).

## 4 | RESULTS AND DISCUSSIONS

### 4.1 | Radiative forcing

The GHG emissions from each location considered (Table 1) were tracked individually over 100 observation years. Figure 4a shows the RF profile comparison for the natural gas and biomass-based heat demand scenarios by location and the influence of GHG emissions due to variation in feedstock and infrastructure choice. Overall, the RF profiles increase or decrease consistently from the 0th year of infrastructure implementation to the 30th year, the end of production. After the 30th observation year, RF is influenced by accumulated GHGs in the atmosphere and additional CO<sub>2</sub> released from unused forest residue decaying naturally. Scenarios with BECCS/CCS show pronounced negative emissions (Figure 4b). Both the 0th and 30th years correspond with a pronounced inflection point in RF for BECCS scenarios. Scenarios with soil carbon sequestration and BECCS stop sequestering CO<sub>2</sub> at the 30th observation year. The coefficient of variation (CV) of RF across the locations per unit heat demand in the 30th observation year is 5% and 6% for NG-CH and NG-DH cases, respectively. Heating scenarios without natural gas pipelines have a CV of 18% DH-BM, 14% DH-W-CW, and 6% DH-W-PHG.

The RF for both HO scenarios is several orders of magnitude greater than all other scenarios at each timestep and is reported separately (Figure S1). The RF in CH-HO is large compared to all DH scenarios due to the CHP electricity



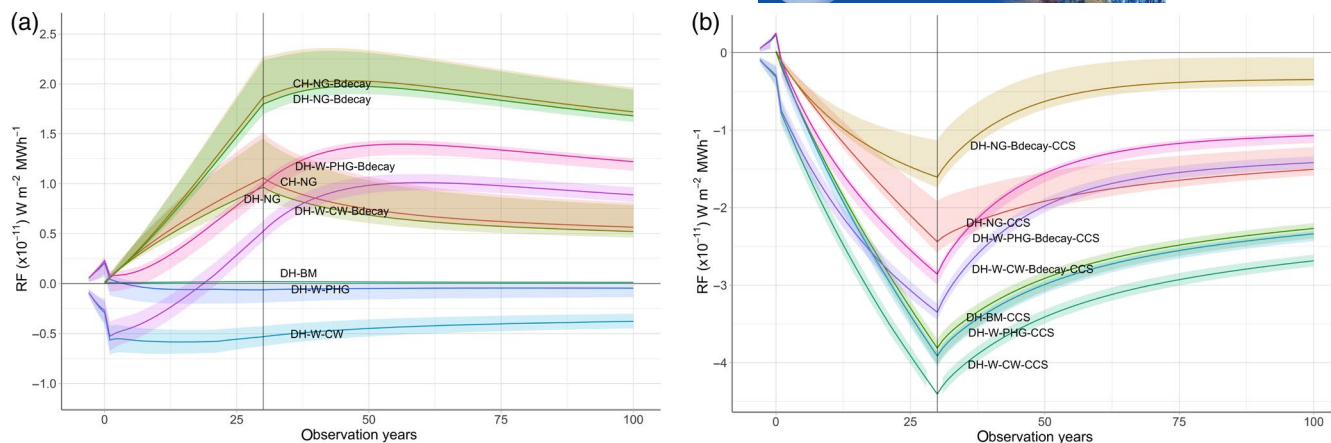


**FIGURE 4** Spatially varying RF ( $\text{W m}^{-2} \text{MWh}^{-1}$ ) as a function of time for the alternative feedstocks and heating infrastructure scenarios, (a) without CCS consideration and (b) with CCS consideration. A soil depth of 100 cm is considered for an accounting of soil carbon sequestration. CCS, carbon capture and storage; CH, conventional heating; DH, district heating; GHG, greenhouse gas; RF, radiative forcing

**TABLE 3** Radiative forcing (RF) values for the various residential heating scenarios at the end of production and observation years

Scenario abbreviation	Median RF at the end of production years <sup>a</sup> ( $\text{W m}^{-2} \text{MWh}^{-1}$ )	Median RF at the end of observation years <sup>a</sup> ( $\text{W m}^{-2} \text{MWh}^{-1}$ )
CH-HO	$5.06 \times 10^{-10}$	$2.63 \times 10^{-10}$
CH-HO-Bdecay	$5.15 \times 10^{-10}$ (2%)	$2.75 \times 10^{-10}$ (5%)
CH-NG	$1.06 \times 10^{-11}$	$5.65 \times 10^{-12}$
CH-NG-Bdecay	$1.87 \times 10^{-11}$ (43%)	$1.72 \times 10^{-11}$ (67%)
DH-NG	$9.66 \times 10^{-12}$	$5.22 \times 10^{-12}$
DH-NG-CCS	$-2.44 \times 10^{-11}$ (353%)	$-1.51 \times 10^{-11}$ (389%)
DH-NG-Bdecay	$1.80 \times 10^{-11}$ (46%)	$1.68 \times 10^{-11}$ (69%)
DH-NG-Bdecay-CCS	$-1.61 \times 10^{-11}$ (189%)	$-3.48 \times 10^{-12}$ (120%)
DH-BM	$1.99 \times 10^{-13}$	$1.26 \times 10^{-13}$
DH-BM-CCS	$-3.81 \times 10^{-11}$ (>500%)	$-2.27 \times 10^{-11}$ (>500%)
DH-W-CW	$-5.29 \times 10^{-12}$	$-3.76 \times 10^{-12}$
DH-W-PHG	$-5.97 \times 10^{-13}$	$-4.37 \times 10^{-13}$
DH-W-CW-Bdecay	$5.27 \times 10^{-12}$ (200%)	$8.90 \times 10^{-12}$ (337%)
DH-W-PHG-Bdecay	$9.96 \times 10^{-12}$ (>500%)	$1.22 \times 10^{-11}$ (>500%)
DH-W-CW-CCS	$-4.41 \times 10^{-11}$ (>500%)	$-2.69 \times 10^{-11}$ (>500%)
DH-W-PHG-CCS	$-3.91 \times 10^{-11}$ (>500%)	$-2.34 \times 10^{-11}$ (>500%)
DH-W-CW-Bdecay-CCS	$-3.35 \times 10^{-11}$ (>500%)	$-1.42 \times 10^{-11}$ (>500%)
DH-W-PHG-Bdecay-CCS	$-2.86 \times 10^{-11}$ (387%)	$-1.07 \times 10^{-11}$ (>500%)

<sup>a</sup>Percentages in parentheses for scenarios with biomass decay show % increase in RF estimate when biomass decay is considered. Percentages in parentheses for scenarios with carbon capture and storage (CCS) show % decrease in RF estimate with respect to non-CCS scenarios. Scenarios with excessive differences are shown as >500%.

credit. Moreover, the biomass decay contribution to CH-HO is insignificant, with the CH-HO and CH-HO-Bdecay approximately overlapping. The RF in the CH-HO scenario is 97% higher in the 30th year than the RF in the CH-NG scenario. When unused forest residue decay is considered, the CH-HO-Bdecay scenario has a 97% higher RF in the 30th

year compared to scenarios with centralized heating with natural gas (CH-NG-Bdecay). We include Table 3, which accompanies Figure 4, to explain the increase or decrease in RF at the end of the production and observation years. One of the features of the DH with willow grown on cropland (DH-W-CW) is that when coupled with CCS (DH-W-CW-CCS), its

RF declines by more than 500%. Moreover, even when forest residue decay is included, the RF for DH with willow grown on cropland and CCS (DH-W-CW-Bdecay-CCS) still declines by more than 500%.

Conventional heating and DH with natural gas have similar RF effects due to the high efficiency of equipment in both infrastructures. When unused forest residue decay is considered, *CH-NG-Bdecay* and *DH-NG-Bdecay* scenarios have a 43% and 46% higher RF in the 30th observation year, respectively. At the 100th observation year, the adverse effect of unused forest residues increases the RF by 67% and 69% for *CH-NG-Bdecay* and *DH-NG-Bdecay* scenarios, respectively. Hence, the environmental cost of not using available forest residue and letting it decay naturally significantly influences the RF performance of natural-gas-based residential heating. For equivalent scenarios of DH with natural gas, implementation of CCS incurs an energy penalty due to additional burning of natural gas, from which 90% of CO<sub>2</sub> emissions are sequestered, showing negative emissions per unit space heating demand (Figure 4b). Using forest residue as feedstock expedites C emissions from forest residue but avoids GHG emissions from fossil fuels. *DH-BM* is 90 times and 4 times lower in RF in the 30th observation year and 133 times and 6 times lower in RF in the 100th observation year, compared to *DH-NG-Bdecay* and *CH-NG-Bdecay*, respectively. There is a tremendous reduction in RF when available forest residues are used for residential heating, replacing natural gas. For forest residue biomass use in the DH scenario with CCS, a large negative RF is observed, which is due to capturing CO<sub>2</sub> emitted from space heating as well as additional forest residues used to satisfy the energy penalty of the CCS infrastructure.

Growing willow feedstock requires 4 initial years for land preparation, where the fourth year overlaps with the installation of DH infrastructure. LUC emissions from converting cropland (CW) to willow immediately increase soil carbon, producing a negative RF; this contrasts with the positive RF caused by LUC emissions from converting pasture, hay, grasslands (PHG) to willow cultivation. Although willow growth contributes to soil carbon sequestration, the benefit of using willow feedstock diminishes for *DH-W-PHG*, compared with *DH-W-CW*. However, both scenarios show negative RF for the 100 observation years. The *DH-W-PHG-Bdecay* and *DH-CW-Bdecay* scenarios, where forest residues are unused and left for natural decay, significantly influence the RF profile. *DH-W-PHG-Bdecay* shows positive RF for all observation years, and *DH-CW-Bdecay* shows positive RF from the 19th observation year. With CCS technology, *DH-W-PHG-CCS* and *DH-W-CW-CCS* both show negative RF for 100 observation years with 50% more RF savings in CW LUC compared to PHG LUC in the 30th observation year. With CCS technology and when forest residues are left to decay naturally, the *DH-W-PHG-Bdecay*, *CCS*, and

*DH-W-CW-Bdecay* stop being RF negative in the 26th and 39th observation years, respectively. Hence, this comparison shows that willow's use for DH has a high carbon-negative potential if LUC is carefully planned and selected only in the absence of available forest residues. Willow feedstock for the DH scenarios for either CW or PHG LUC are lower in RF than forest residue scenarios.

There is an additional negative RF for the DH scenarios with CCS attributed to the capture of 90% of CO<sub>2</sub> emissions from additional feedstock needed to operate the CCS infrastructure, which may not be considered a benefit. CCS implementation significantly reduces (and renders negative) net RF across the timeline for all DH scenarios (Figure 4b). The much lower RF for scenarios with CCS is attributed to the additional feedstocks consumed by CCS operation; however, this negative RF may be considered a result of sub-optimal use of biomass resources. Hence, CCS may not be feasible when biomass resources are limited.

## 4.2 | Global warming factor

While the RF metric estimates the temporally varying environmental impact of the different space heating scenarios, GWF helps to quantify the fraction change in RF compared to one unit pulse emission allowing comparison to the baseline heating oil scenario. Considering *CH-HO* as the baseline scenario, we calculate the GWF over the 100 observation years. A negative GWF indicates that the scenario's CRF effect is lower than the baseline scenario. The absolute value of the GWF shows the number of times CRF is higher than a 1 kg CO<sub>2</sub> pulse emission for every 30 production years. Figure 5 shows the GWF over 100 observation years for selected scenarios. All scenarios are not shown as they overlap. Negative GWF is seen across all scenarios, showing a significant advantage over the *CH-HO* baseline scenario across the observation years, except for DH with willow grown on PHG. The willow use causing LUC scenario initially sees high GWF for the first year due to LUC. It immediately becomes negative, from the second production year, as soil carbon sequestration and avoidance of fossil emission benefits are established. Hence, the GWF metric further highlights the improved environmental performance of alternative space heating scenarios, justifying the transition from CH oil-based infrastructure to natural gas or biomass-based space heating infrastructure.

## 4.3 | Willow SOC scenarios

Willow production consists of 4 years where the first year involves land preparations and the subsequent 3 years involve planting willow crop rotations. GHG emissions

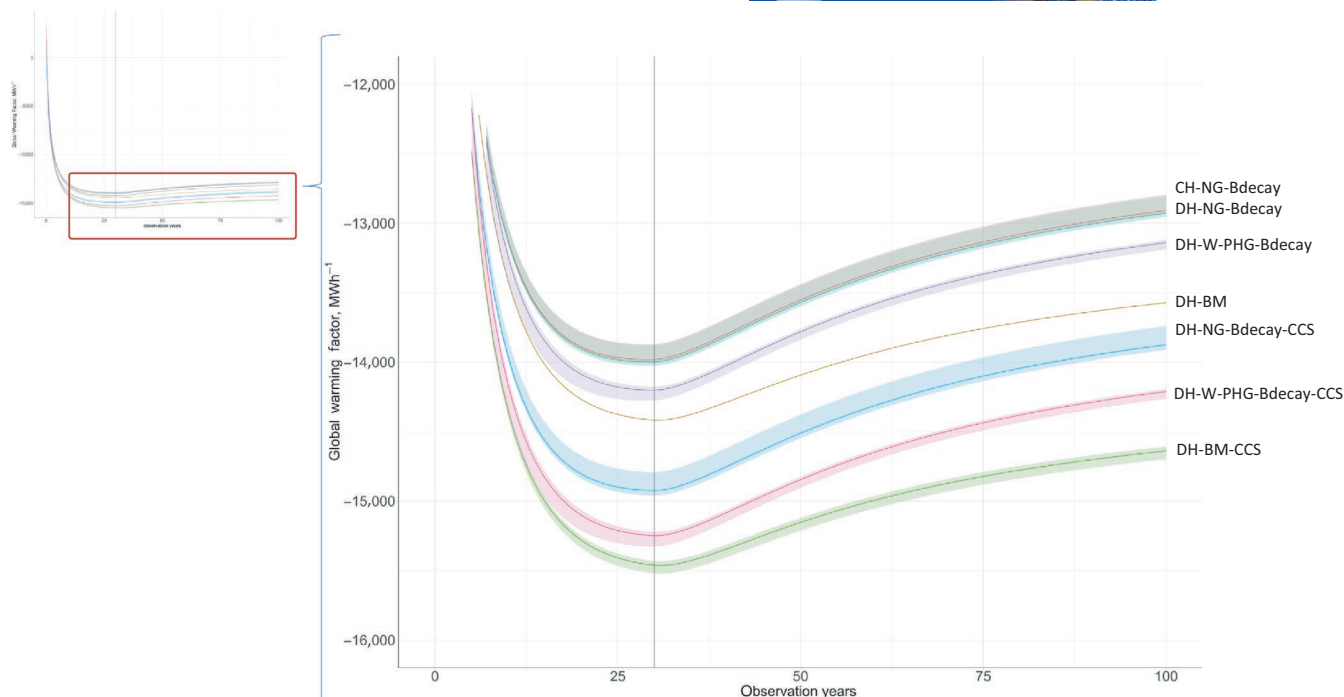
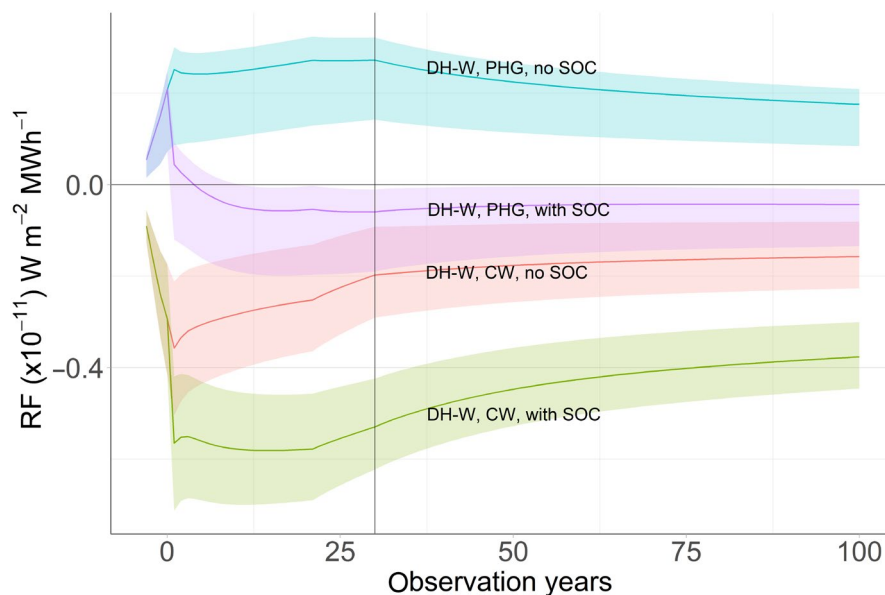


**FIGURE 5** Global warming factor for the compared scenarios with their spatial uncertainty. CCS, carbon capture and storage; CH, conventional heating; DH, district heating

**FIGURE 6** Comparison of presence and absence of soil carbon sequestration effects on spatially varying RF ( $\text{W m}^{-2} \text{MWh}^{-1}$ ) estimates for willow feedstock-based district heating infrastructure. DH, district heating; RF, radiative forcing



in the fourth year relate to DH infrastructure installation. The next 30 years consider DH-production-based GHG emissions. The climate change benefit of soil carbon sequestration, contributing to an increase in soil organic carbon from growing willow, is simulated from the fifth production year. Considering soil carbon sequestration for temporal accounting of RF from growing short-rotation willow crop significantly impacts the temporal emissions profile over the 104 observation years (Figure 6). The advantage of growing willow on cropland is that

its negative RF is pronounced due to an increase in soil organic carbon from growing willow. If there were no soil carbon sequestration, DH with willow grown on pasture, hay, and grassland could not be classified as a RF-negative scenario.

The land selection decision for willow cultivation is most significant when using the feedstock in DH infrastructure planning to minimize the yearly GHG emissions for 104 observed years. Both biomass cases have lower RF than natural gas. The additional benefit of short-rotation

feedstock crops can be harnessed by targeting appropriate lands at the beginning of the project.

## 5 | CONCLUSION

Radiative forcing as a metric to address temporally asynchronous life cycle GHG emissions elucidates the timing of climate change impacts related to infrastructure installation, fuel combustion, CO<sub>2</sub> uptake by soils used to grow biomass, and different biomass sources. Thus, it can support the selection of residential space heating investment to mitigate climate change. The RF metric enables evaluating the climate change impact of space heating technology at annual timesteps in a planning horizon. Spikes or inflection points in GHG emissions can occur at different junctures of a heating infrastructure life cycle, which can have a prolonged climatic effect. Information on the climatic effects of those spikes is lost when aggregating time-series GHG emissions data. Our analysis compares conventional and district space heating scenarios with alternative feedstocks while preserving temporal information over the production timeline. Despite the initial carbon cost from infrastructure investment into DH, forest residues and short-rotation willow reduce GHG emissions as early as the fifth production year when soil carbon sequestration benefits are realized, compared to heating oil scenarios, the dominant space-heating energy source in the U.S. Northeast. Using CCS technology to sequester CO<sub>2</sub> from flue gas is effective in reducing RF from space heating; however, CCS technology itself incurs a significant energy penalty and additional biomass consumption beyond supplying heat and power. This should be taken into consideration if planning its implementation.

One limitation of this work is that we consider a total of 20 locations, 10 for natural gas, and 10 for forest residue use, in residential heating based on economically feasible biomass availability. While our heat demand estimation and boundary assumptions related to heating infrastructure (central or DH) provided a good estimate of variability related to the quantity of energy supplied, it does not estimate sub-variables related to forest residues, namely, decay rates over the 30 years of operation and 100-year time horizon of RF estimation. This imitation could be improved with better location-specific data on biomass decay and soil carbon change and sequestration for climate conditions in the Northeastern United States. Further analysis of parameter uncertainties in the time-dependent RF model could also consider an optimization approach to select low GHG emitting biomass feedstocks (Field et al., 2018; Kar et al., 2020). If combined with multi-objective optimization, such an approach can optimize space

heating alternatives while considering temporal variations in soil properties, feedstock availability, and changes in temporal heat demand while using biomass feedstocks to mitigate atmospheric CO<sub>2</sub>.

## ACKNOWLEDGEMENTS

This project was supported by Agriculture and Food Research Initiative Competitive Grant No. 2012-68005-19703 from the USDA National Institute of Food and Agriculture. Saurajyoti Kar would like to thank Drexel University's College of Engineering teaching fellowship for support during the duration of this work.

## CONFLICT OF INTEREST

The authors declare no conflict of interest for this work.

## DATA AVAILABILITY STATEMENT

The program files and the input data file are published as Mendeley data (Kar et al., 2019). The program files can be run in the R programming environment with the input code file to re-perform the simulation analyses. The details on the stepwise mathematical formulation and analysis can be found in the Supporting Information-A document.


## ORCID

Saurajyoti Kar  <https://orcid.org/0000-0001-9264-4599>

Pieter Billen  <https://orcid.org/0000-0003-3546-0157>

Sheng Yang  <https://orcid.org/0000-0002-6771-3174>

Timothy A. Volk  <https://orcid.org/0000-0002-6969-9281>

Sabrina Spatari  <https://orcid.org/0000-0001-7243-9993>

## REFERENCES

- Alvarez, R. A., Zavala-Araiza, D., Lyon, D. R., Allen, D. T., Barkley, Z. R., Brandt, A. R., Davis, K. J., Herndon, S. C., Jacob, D. J., Karion, A., Kort, E. A., Lamb, B. K., Lauvaux, T., Maasakkers, J. D., Marchese, A. J., Omara, M., Pacala, S. W., Peischl, J., Robinson, A. L., ... Hamburg, S. P. (2018). Assessment of methane emissions from the U.S. oil and gas supply chain. *Science*, eaar7204. <https://doi.org/10.1126/science.aar7204>
- Björnebo, L. (2015). *Life cycle and economic evaluation of replacing conventional heating methods with biomass and natural gas-based district heating in the northeastern United States*. Linköping University.
- Björnebo, L., Spatari, S., & Gurian, P. L. (2018). A greenhouse gas abatement framework for investment in district heating. *Applied Energy*, 211, 1095–1105. <https://doi.org/10.1016/j.apenergy.2017.12.003>
- Brandt, A. R., Heath, G. A., & Cooley, D. (2016). Methane leaks from natural gas systems follow extreme distributions. *Environmental Science & Technology*, 50(22), 12512–12520. <https://doi.org/10.1021/acs.est.6b04303>
- CARB. (2012). Low carbon fuel standard. In *California code of regulations*. California Air Resource Board.



- CARB. (2013). Regulation of fuels and fuel additives: 2013 renewable fuel standards. In *Federal register* (Vol. 78, Issue 158, pp. 49794–49830).
- Cherubini, F., Huijbregts, M., Kindermann, G., Van Zelm, R., Van Der Velde, M., Stadler, K., & Strömman, A. H. (2016). Global spatially explicit CO<sub>2</sub> emission metrics for forest bioenergy. *Scientific Reports*, 6(1), 20186. <https://doi.org/10.1038/srep20186>
- Cherubini, F., Peters, G. P., Berntsen, T., Strömman, A. H., & Hertwich, E. (2011). CO<sub>2</sub> emissions from biomass combustion for bioenergy: Atmospheric decay and contribution to global warming. *GCB Bioenergy*, 3(5), 413–426. <https://doi.org/10.1111/j.1757-1707.2011.01102.x>
- Cherubini, F., Strömman, A. H., & Ulgiati, S. (2011). Influence of allocation methods on the environmental performance of biorefinery products—A case study. *Resources, Conservation and Recycling*, 55(11), 1070–1077. <https://doi.org/10.1016/j.rescon.2011.06.001>
- Chu, S., & Majumdar, A. (2012). Opportunities and challenges for a sustainable energy future. *Nature*, 488, 294. <https://doi.org/10.1038/nature11475>
- Davidson, E. A., & Ackerman, I. L. (1993). Changes in soil carbon inventories following cultivation of previously untilled soils stable. *Biogeochemistry*, 20(3), 161–193. <https://doi.org/10.1007/BF00000786>
- Dias, G. M., Ayer, N. W., Kariyapperuma, K., Thevathasan, N., Gordon, A., Sidders, D., & Johannesson, G. H. (2017). Life cycle assessment of thermal energy production from short-rotation willow biomass in Southern Ontario, Canada. *Applied Energy*, 204, 343–352. <https://doi.org/10.1016/j.apenergy.2017.07.051>
- Dunn, J. B., Mueller, S., Kwon, H., & Wang, M. Q. (2013). Land-use change and greenhouse gas emissions from corn and cellulosic ethanol. *Biotechnology for Biofuels*, 6(1), 51. <https://doi.org/10.1186/1754-6834-6-51>
- Dunn, J. B., Qin, Z., Steffen, M., Kwon, H.-y., Wander, M. M., & Michael, W. (2017). *Carbon calculator for land use change from biofuels production (CCLUB)* (Issue September). Argonne National Laboratory. <https://doi.org/10.2172/1414292>
- European Commission. (2018). *More growth and jobs: EU invests €873 million in clean energy infrastructure*. [http://europa.eu/rapid/press-release\\_IP-18-383\\_en.htm](http://europa.eu/rapid/press-release_IP-18-383_en.htm)
- Field, J. L., Evans, S. G., Marx, E., Easter, M., Adler, P. R., Dinh, T., Willson, B., & Paustian, K. (2018). High-resolution technoeological modelling of a bioenergy landscape to identify climate mitigation opportunities in cellulosic ethanol production. *Nature Energy*, 3(3), 211–219. <https://doi.org/10.1038/s41560-018-0088-1>
- Forster, P., Ramaswamy, V., Artaxo, P., Berntsen, T., Betts, R., Fahey, D. W., Haywood, J., Lean, J., Lowe, D. C., Myhre, G., Nganga, J., Prinn, R., Raga, G., Schulz, M., & Van Dorland, R. (2007). Changes in atmospheric constituents and in radiative forcing. In S. Solomon, D. Qin, M. Manning, Z. Chen, M. Marquis, K. B. Averyt, M. Tignor, & H. L. Miller (Eds.), *Climate change 2007: The physical science basis, contribution of working group I to the fourth assessment report of the intergovernmental panel on climate change* (p. 996). Cambridge University Press. <http://www.ipcc.ch/pdf/assessment-report/ar4/wg1/ar4-wg1-chapter2.pdf>
- Fuss, S., Lamb, W. F., Callaghan, M. W., Hilaire, J., Creutzig, F., Amann, T., Beringer, T., de Oliveira Garcia, W., Hartmann, J., Khanna, T., Luderer, G., Nemet, G. F., Rogelj, J., Smith, P., Vicente, J. L. V., Wilcox, J., del Mar Zamora Dominguez, M., & Minx, J. C. (2018). Negative emissions—Part 2: Costs, potentials and side effects. *Environmental Research Letters*, 13(6), 063002. <https://doi.org/10.1088/1748-9326/aabf9f>
- Gelfand, I., Hamilton, S. K., Kravchenko, A. N., Jackson, R. D., Thelen, K. D., & Robertson, G. P. (2020). Empirical evidence for the potential climate benefits of decarbonizing light vehicle transport in the U.S. with bioenergy from purpose-grown biomass with and without BECCS. *Environmental Science & Technology*, 54(5), 2961–2974. <https://doi.org/10.1021/acs.est.9b07019>
- Gelfand, I., Sahajpal, R., Zhang, X., Izaurrealde, R. C., Gross, K. L., & Robertson, G. P. (2013). Sustainable bioenergy production from marginal lands in the US Midwest. *Nature*, 493(7433), 514–517. <https://doi.org/10.1038/nature11811>
- Harmon, M. E., Krankina, O. N., & Sexton, J. (2000). Decomposition vectors: A new approach to estimating woody detritus decomposition dynamics. *Canadian Journal of Forest Research*, 30, 76–84. <https://doi.org/10.1139/x99-187>
- Havlik, P., Schneider, U. A., Schmid, E., Böttcher, H., Fritz, S., Skalský, R., Aoki, K., Cara, S. D., Kindermann, G., Kraxner, F., Leduc, S., McCallum, I., Mosnier, A., Sauer, T., & Obersteiner, M. (2011). Global land-use implications of first and second generation biofuel targets. *Energy Policy*, 39(10), 5690–5702. <https://doi.org/10.1016/j.enpol.2010.03.030>
- Heller, M. C., Keoleian, G. A., & Volk, T. A. (2003). Life cycle assessment of a willow bioenergy cropping system. *Biomass and Bioenergy*, 25(2), 147–165. [https://doi.org/10.1016/S0961-9534\(02\)00190-3](https://doi.org/10.1016/S0961-9534(02)00190-3)
- Henning, D. (1998). Cost minimization for a local utility through CHP, heat storage and load management. *International Journal of Energy Research*, 22(8), 691–713. [https://doi.org/10.1002/\(SICI\)1099-114X\(19980625\)22:8<691::AID-ER395>3.0.CO;2-E](https://doi.org/10.1002/(SICI)1099-114X(19980625)22:8<691::AID-ER395>3.0.CO;2-E)
- Henning, D. (1999). *Optimisation of local and national energy systems—Development and use of the MODEST model*. Linköping University.
- Henning, D., Amiri, S., & Holmgren, K. (2006). Modelling and optimisation of electricity, steam and district heating production for a local Swedish utility. *European Journal of Operational Research*, 175(2), 1224–1247. <https://doi.org/10.1016/j.ejor.2005.06.026>
- Jørgensen, S. V., & Hauschild, M. Z. (2013). Need for relevant timescales when crediting temporary carbon storage. *International Journal of Life Cycle Assessment*, 18(4), 747–754. <https://doi.org/10.1007/s11367-012-0527-3>
- Kaito, C., Ito, A., Kimura, S., Kimura, Y., Saito, Y., & Nakada, T. (2014). *Fifth Assessment Report (AR5)*. IPCC. [https://doi.org/10.1016/S0022-0248\(00\)00575-3](https://doi.org/10.1016/S0022-0248(00)00575-3)
- Kar, S., Billen, P., Katz, B., Yang, S., Volk, T. A., Björnebo, L., & Spatarì, S. (2019). *Computer program and input data set for performing comparative temporal analyses of heating infrastructure scenarios*. Mendeley Data. <https://doi.org/10.17632/h7fcp ytx3g.2>
- Kar, S., Riazi, B., Gurian, P. L., Spatarì, S., Adler, P. R., & Parton, W. J. (2020). An optimization framework to identify key management strategies for improving biorefinery performance: A case study of winter barley production. *Biofuels, Bioproducts and Biorefining*, 14(6), 1296–1312. <https://doi.org/10.1002/bbb.2141>
- Kellndorfer, J., Walker, W., LaPoint, E., Bishop, J., Cormier, T., Fiske, G., Hoppus, M., Kirsch, K., & Westfall, J. (2013). *NACP*

- aboveground biomass and carbon baseline data, V.2 (NBCD 2000), U.S.A., 2000. [https://daac.ornl.gov/NACP/guides/NBCD\\_2000\\_V2.html](https://daac.ornl.gov/NACP/guides/NBCD_2000_V2.html)
- Kendall, A., Chang, B., & Sharpe, B. (2009). Accounting for time-dependent effects in biofuel life cycle greenhouse gas emissions calculations. *Environmental Science and Technology*, 43(18), 7142–7147. <https://doi.org/10.1021/es900529u>
- Kløverpris, J. H., & Mueller, S. (2013). Baseline time accounting: Considering global land use dynamics when estimating the climate impact of indirect land use change caused by biofuels. *The International Journal of Life Cycle Assessment*, 18(2), 319–330. <https://doi.org/10.1007/s11367-012-0488-6>
- Kunze, C., & Spliethoff, H. (2012). Assessment of oxy-fuel, pre- and post-combustion-based carbon capture for future IGCC plants. *Applied Energy*, 94, 109–116. <https://doi.org/10.1016/j.apenergy.2012.01.013>
- Kwon, H. Y., & Hudson, R. J. M. (2010). Quantifying management-driven changes in organic matter turnover in an agricultural soil: An inverse modeling approach using historical data and a surrogate CENTURY-type model. *Soil Biology and Biochemistry*, 42(12), 2241–2253. <https://doi.org/10.1016/j.soilbio.2010.08.025>
- Langholtz, M. H., Stokes, B. J., & Eaton, L. M. (2016). *2016 Billion-Ton report: Advancing domestic resources for a thriving bioeconomy*. <https://doi.org/10.2172/1271651>
- Levasseur, A., Cavalett, O., Fuglestedt, J. S., Gasser, T., Johansson, D. J. A., Jørgensen, S. V., Rauegi, M., Reisinger, A., Schivley, G., Strømman, A., Tanaka, K., & Cherubini, F. (2016). Enhancing life cycle impact assessment from climate science: Review of recent findings and recommendations for application to LCA. *Ecological Indicators*, 71, 163–174. <https://doi.org/10.1016/j.ecolind.2016.06.049>
- Levasseur, A., Lesage, P., & Margni, M. (2010). Dynamic LCA and its application to global warming impact assessment. *Time*, 44(8), 3169–3174. <https://doi.org/10.1021/es9030003>
- McKendry, P. (2002). Energy production from biomass (part 1): Overview of biomass. *Bioresource Technology*, 83, 37–46. [https://doi.org/10.1016/S0960-8524\(01\)00119-5](https://doi.org/10.1016/S0960-8524(01)00119-5)
- McManus, M. C. (2010). Life cycle impacts of waste wood biomass heating systems: A case study of three UK based systems. *Energy*, 35(10), 4064–4070. <https://doi.org/10.1016/j.energy.2010.06.014>
- Metz, B., Davidson, O., De Coninck, H., Loos, M., & Meyer, L. (2005). *Carbon dioxide capture and storage; IPCC, 2005: IPCC special report on carbon dioxide capture and storage*. Cambridge University Press.
- Middleton, R. S., & Bielicki, J. M. (2009). A scalable infrastructure model for carbon capture and storage: SimCCS. *Energy Policy*, 37(3), 1052–1060. <https://doi.org/10.1016/j.enpol.2008.09.049>
- Moser, P., Schmidt, S., & Stahl, K. (2011). Investigation of trace elements in the inlet and outlet streams of a MEA-based post-combustion capture process results from the test programme at the Niederaussem pilot plant. *Energy Procedia*, 4(2010), 473–479. <https://doi.org/10.1016/j.egypro.2011.01.077>
- Myhre, G., Shindell, D., Bréon, F.-M., Collins, W., Fuglestedt, J., Huang, J., Koch, D., Lamarque, J.-F., Lee, D., Mendoza, B., Nakajima, T., Robock, A., Stephens, G., Takemura, T., & Zhang, H. (2013). Anthropogenic and natural radiative forcing. In T. F. Stocker (Ed.), *Climate change 2013: The physical science basis. Contribution of working group I to the fifth assessment report of the intergovernmental panel on climate change* (pp. 659–740). IPCC.
- O'Hare, M., Plevin, R. J., Martin, J. I., Jones, A. D., Kendall, A., & Hopson, E. (2009). Proper accounting for time increases crop-based biofuels' greenhouse gas deficit versus petroleum. *Environmental Research Letters*, 4(2), 24001. <https://doi.org/10.1088/1748-9326/4/2/024001>
- Pacaldo, R. S., Volk, T. A., & Briggs, R. D. (2013). Greenhouse gas potentials of shrub willow biomass crops based on below- and aboveground biomass inventory along a 19-year chronosequence. *Bioenergy Research*, 6(1), 252–262. <https://doi.org/10.1007/s12155-012-9250-y>
- Palviainen, M., Finér, L., Kurka, A.-M., Mannerkoski, H., Piirainen, S., & Starr, M. (2004). Decomposition and nutrient release from logging residues after clear-cutting of mixed boreal forest. *Plant and Soil*, 263(1), 53–67. <https://doi.org/10.1023/B:PLSO.0000047718.34805.fb>
- Parajuli, R., Sperling, K., & Dalgaard, T. (2015). Environmental performance of Miscanthus as a fuel alternative for district heat production. *Biomass and Bioenergy*, 72, 104–116. <https://doi.org/10.1016/j.biombioe.2014.11.011>
- Paustian, K., Parton, W. J., & Persson, J. (1992). Modeling soil organic matter in organic-amended and nitrogen-fertilized long-term plots. *Soil Science Society of America Journal*, 56(2), 476–488. <https://doi.org/10.2136/sssaj1992.03615995005600020023x>
- Pedersen, P., Boote, K. J., Jones, J. W., & Lauer, J. G. (2004). Modifying the CROPGRO-Soybean model to improve predictions for the upper Midwest. *Agronomy Journal*, 96(2), 556–564. <https://doi.org/10.2134/agronj2004.5560>
- Pingoud, K., Ekholm, T., & Savolainen, I. (2012). Global warming potential factors and warming payback time as climate indicators of forest biomass use. *Mitigation and Adaptation Strategies for Global Change*, 17(4), 369–386. <https://doi.org/10.1007/s11027-011-9331-9>
- Pinsonnault, A., Lesage, P., Levasseur, A., & Samson, R. (2014). Temporal differentiation of background systems in LCA: Relevance of adding temporal information in LCI databases. *The International Journal of Life Cycle Assessment*, 19(11), 1843–1853. <https://doi.org/10.1007/s11367-014-0783-5>
- Pourhashem, G., Adler, P. R., & Spataro, S. (2016). Time effects of climate change mitigation strategies for second generation biofuels and co-products with temporary carbon storage. *Journal of Cleaner Production*, 112, 2642–2653. <https://doi.org/10.1016/j.jclepro.2015.09.135>
- R Core Team. (2018). *R: A language and environment for statistical computing*. R Foundation for Statistical Computing. <https://www.r-project.org/>
- Rhodes, J. S., & Keith, D. W. (2005). Engineering economic analysis of biomass IGCC with carbon capture and storage. *Biomass and Bioenergy*, 29(6), 440–450. <https://doi.org/10.1016/j.biombioe.2005.06.007>
- Rubin, E. S., & Zhai, H. (2012). The cost of carbon capture and storage for natural gas combined cycle power plants. *Environmental Science & Technology*, 46(6), 3076–3084. <https://doi.org/10.1021/es204514f>
- Saint-Pierre, A., & Mancarella, P. (2014). *Techno-economic assessment of flexible combined heat and power plant with carbon capture and storage*. 2014 Power systems computation conference (pp. 1–7). <https://doi.org/10.1109/PSCC.2014.7038449>
- Schivley, G., Ingwersen, W. W., Marriott, J., Hawkins, T. R., & Skone, T. J. (2015). Identifying/quantifying environmental trade-offs

- inherent in GHG reduction strategies for coal-fired power. *Environmental Science and Technology*, 49(13), 7562–7570. <https://doi.org/10.1021/acs.est.5b01118>
- Schwietzke, S., Griffin, W. M., & Matthews, H. S. (2011). Relevance of emissions timing in biofuel greenhouse gases and climate impacts. *Environmental Science & Technology*, 45(19), 8197–8203. <https://doi.org/10.1021/es2016236>
- Searchinger, T., Heimlich, R., Houghton, R. A., Dong, F., Elobeid, A., Fabiosa, J., Tokgoz, S., Hayes, D., & Yu, T.-H. (2008). Use of U.S. croplands for biofuels increases greenhouse gases through emissions from land-use change. *Science*, 319(5867), 1238–1240. <https://doi.org/10.1126/science.1151861>
- Shine, K. P. (2009). The global warming potential—the need for an interdisciplinary retrieval. *Climatic Change*, 96(4), 467–472. <https://doi.org/10.1007/s10584-009-9647-6>
- Singh, B., Strömman, A. H., & Hertwich, E. (2011). Life cycle assessment of natural gas combined cycle power plant with post-combustion carbon capture, transport and storage. *International Journal of Greenhouse Gas Control*, 5(3), 457–466. <https://doi.org/10.1016/j.ijggc.2010.03.006>
- Strassmann, K. M., & Joos, F. (2018). The Bern Simple Climate Model (BernSCM) v1.0: An extensible and fully documented open-source re-implementation of the Bern reduced-form model for global carbon cycle-climate simulations. *Geoscientific Model Development*, 11(5), 1887–1908. <https://doi.org/10.5194/gmd-11-1887-2018>
- USEIA. (2015). *U.S. Energy Information Administration, Forms EIA-457A, C, D, E, F, G of the 2015 residential energy consumption survey*. <https://www.eia.gov/consumption/residential/data/2015/index.php?view=consumption#byEndusesbyfuel>
- USEIA. (2015). *Use of heating oil*. Administration, U.S. Energy Information.
- USEPA. (2020). *Greenhouse gas inventory guidance—Direct emissions from stationary combustion sources*. <https://www.epa.gov/sites/production/files/2020-12/documents/stationaryemissions.pdf>
- Vávřová, P., Penttilä, T., & Laiho, R. (2009). Decomposition of Scots pine fine woody debris in boreal conditions: Implications for estimating carbon pools and fluxes. *Forest Ecology and Management*. <https://doi.org/10.1016/j.foreco.2008.09.017>
- Verwijst, T. (2001). Willows: An underestimated resource for environment and society. *The Forestry Chronicle*, 77(2), 281–285. <https://doi.org/10.5558/tfc77281-2>
- Volk, T. A., Heavey, J. P., & Eisenbies, M. H. (2016). Advances in shrub-willow crops for bioenergy, renewable products, and environmental benefits. *Food and Energy Security*, 5(2), 97–106. <https://doi.org/10.1002/fes3.82>
- Volkart, K., Bauer, C., & Boulet, C. (2013). Life cycle assessment of carbon capture and storage in power generation and industry in Europe. *International Journal of Greenhouse Gas Control*, 16, 91–106. <https://doi.org/10.1016/j.ijggc.2013.03.003>
- Wilson, T. O., McNeal, F. M., Spatari, S., Abler, G. D., & Adler, P. R. (2012). Densified biomass can cost-effectively mitigate greenhouse gas emissions and address energy security in thermal applications. *Environmental Science and Technology*, 46(2), 1270–1277. <https://doi.org/10.1021/es202752b>
- Zumkehr, A., & Campbell, J. E. (2013). Historical U.S. cropland areas and the potential for bioenergy production on abandoned croplands. *Environmental Science & Technology*, 47(8), 3840–3847. <https://doi.org/10.1021/es3033132>
- Zuwała, J. (2012). Life cycle approach for energy and environmental analysis of biomass and coal co-firing in CHP plant with back-pressure turbine. *Journal of Cleaner Production*, 35, 164–175. <https://doi.org/10.1016/j.jclepro.2012.06.001>

## SUPPORTING INFORMATION

Additional supporting information may be found online in the Supporting Information section.

**How to cite this article:** Kar, S., Billen, P., Björnebo, L., Katz, B., Yang, S., Volk, T. A., & Spatari, S. (2021). Effects of greenhouse gas emissions timing on alternative biomass and fossil energy sources for district heating. *GCB Bioenergy*, 00, 1–15. <https://doi.org/10.1111/gcbb.12890>